

# The Response Surface Method as an Experimental Design Technique to Explore and Model the Performance of Corrosion Inhibitors

A. Kosari,\* A. Davoodi,†\* M.H. Moayed,\* and R. Gheshlaghi\*\*

## ABSTRACT

Numerous environmental factors strongly affect performance of inhibitors. Therefore, many experimental tests and much time are needed to fully explore the inhibitor performance in various conditions. This paper introduces the response surface method using central composite face-centered design as a method in order to explore and mathematically model the inhibitors' behavior in different working conditions. Also, this method provides the ability of significantly decreasing the number of experiments. In this study, as an example, the effect of temperature, hydrochloric acid, and inhibitor concentrations on inhibitive behavior of 4-aminophenyl disulfide for mild steel was examined. Further, two mathematical models were established to estimate mild steel corrosion rate in the inhibited and uninhibited solutions. Analysis of variance was applied to check the adequacy of the models. Finally, the Langmuir adsorption energy was calculated using the acquired models. The results showed that, despite the inhibitor efficiency changes in various conditions, the adsorption type into metal is an invariable parameter.

**KEY WORDS:** inhibitor, mild steel, modeling, polarization, response surface method, temperature

## INTRODUCTION

Corrosion is known as a serious and challenging problem faced by various industries.<sup>1-9</sup> The use of organic inhibitors is recognized as a practical method to reduce the corrosion rate in many industrial parts.<sup>4,10-13</sup> Therefore, a wide range of research has been performed to introduce new compounds that are more efficient and cost effective.<sup>4,7,10,12-19</sup> There are several factors like the nature of metal, aggressive ions concentration, pH value, temperature, immersion time, hydrodynamic flow, etc., that can strongly affect inhibitors' performance.<sup>6,11</sup> Thus, a large number of experiments are needed to thoroughly evaluate the effect of various factors on the inhibitive performance of a considered compound. In general, the method of testing one factor at a time is generally used as an alternative in order to reduce the number of experiments. For instance, the effect of inhibitor concentration is first examined at room temperature to find the optimum concentration and then the temperature effect is investigated at a constant inhibitor concentration. In this respect, the probable interaction between factors, which gives valuable information on inhibitor performance, will not be detected in detail.

Experimental design methods are a collection of mathematical and statistical techniques helpful for developing, improving, and optimizing the processes.<sup>20</sup> They can be used extensively to evaluate the relative significance of several affecting factors even in the presence of complex interactions.<sup>21</sup> The main objective of experimental design methods is to determine

Submitted for publication: November 30, 2014. Revised and accepted: March 30, 2015. Preprint available online: March 31, 2015. <http://dx.doi.org/10.5006/1578>.

† Corresponding author. E-mail: a.davodi@um.ac.ir.

\* Materials and Metallurgical Engineering Department, Faculty of Engineering, Ferdowsi University of Mashhad, Mashhad 91775-1111, Iran.

\*\* Chemical Engineering Department, Faculty of Engineering, Ferdowsi University of Mashhad, Iran.

the optimum operational conditions of the system or a region that satisfies the operating specifications. Furthermore, design of experiments is the most efficient approach for organizing experimental work.<sup>22</sup> Experimental design can reduce the number of experimental runs required to determine the effect of changing variables of one process. Another benefit of the design of experiments is that it allows the effect of one variable to be investigated at several levels of other factors.<sup>22</sup> It selects a diverse and representative set of experiments in which all factors are independent of each other, despite being varied simultaneously.<sup>23-26</sup> The results can reveal the importance of all factors and their interactions, and additionally, the outcomes can be summarized as informative plots.<sup>26</sup> In this way, response surface method (RSM) is known as a statistical and mathematical method that is useful for modeling and analyzing engineering problems.<sup>27-29</sup> RSM also quantifies the relationship between the controllable input parameters and the obtained response.<sup>27,30-31</sup> It can be employed to evaluate the relative significance of several affecting factors even in the presence of complex interactions.<sup>22,26</sup> Basically, the main objective of RSM is to determine the optimum operational conditions of the process or to establish a region that satisfies the operating specifications.<sup>29-30,32-34</sup>

In the present study, RSM using central composite face-centered (CCFD) design was introduced as a practical method to explore and model the inhibitive performance of compounds in various environmental conditions. As an example, the effect of temperature, hydrochloric acid, and inhibitor concentrations on the inhibitive behavior of 4-aminophenyl disulfide (4ATP) for mild steel was examined. Corrosion current density estimated by potentiodynamic polarization technique was considered as a response. Further, two mathematical models were established in order to estimate mild steel corrosion rate in the inhibited and uninhibited solutions. Analysis of variance (ANOVA) was applied to investigate the adequacy of model parameters. Using the obtained mathematical models, the inhibitor efficiency and adsorption energy were calculated in different conditions.

## EXPERIMENTAL PROCEDURES

The inhibitor was 4ATP and was synthesized according to the procedure presented in this reference.<sup>35</sup> The working electrode was selected from a ST37 steel rod (UNS K02401)<sup>(1)</sup> with a chemical composition (in wt%) as follows: 0.16% C, 1.3% Mn, 0.04% S, 0.031% P, and Fe as balance. The sample was then cold mounted in a self-cure epoxy resin, resulting in a 1 cm<sup>2</sup> exposed area. A saturated calomel electrode

and a platinum wire were used as reference and auxiliary electrodes, respectively. In order to estimate the corrosion rate (herein response variable), potentiodynamic polarization was performed in the range of -250 mV to +250 mV around the corrosion potential at a sweep rate of 60 mV/min using a Gill AC<sup>†</sup> laboratory potentiostat (ACM Instruments). The corrosion current densities were calculated by Tafel extrapolation of polarization curves. Prior to potentiodynamic polarization, in order to approach steady state, the samples were held in the corrosive solutions for the duration of 45 min, and the corrosion potentials were recorded. Before each electrochemical measurement, the specimen was mechanically ground up to 1000 grit emery paper, then washed in deionized water and immediately dried with air flow. The electrolytes, aqueous solutions containing various HCl concentrations, were prepared using Merck<sup>†</sup> reagent and distilled water. The temperature was controlled by means of a water bath with  $\pm 1^\circ\text{C}$  accuracy. The electrochemical cell was a 250 mL beaker that was open to air.

## STATISTICAL ANALYSIS

The statistical analysis of the results was performed with Design Expert<sup>†</sup> (Version 7.0) statistical software. In order to analyze the experimental data, multiple regression analyses through the least square method were used. The ANOVA combined with Fisher's statistical test (F-test) were used to evaluate the significance of terms. The regression coefficients of all the terms including linear, quadratic, and interaction involved in the model were analyzed by generating ANOVA tables. The fit of models was checked by calculating coefficient of determination ( $R^2$ ), adjusted coefficient of determination ( $R^2_{\text{adj}}$ ), and predicted coefficient of determination ( $R^2_{\text{pre}}$ ). After checking the models adequacy, surface plots were constructed to evaluate the relationship between the independent variables and the response.

## DESIGN OF EXPERIMENTS AND ANALYZING DATA

### *Inhibited Solutions*

Temperature (called  $X_2$ ) and inhibitor concentration (named  $X_3$ ) are the most important factors affecting inhibitive performance of organic compounds.<sup>10,18-19,35</sup> In this work, the temperature range and inhibitor concentration were considered to be varied from 25°C to 45°C and from 25 mg/L to 200 mg/L (ppm), respectively. In addition, acid concentration (labeled  $X_1$ ), which represented both pH value and aggressive ion concentration, was considered in the range of 0.1 M to 1 M. It should be noted that the main objective of this study was to introduce RSM for inhibitors studies, not to be an in depth study on the inhibitive performance of 4ATP. Thus, other fac-

<sup>(1)</sup> UNS numbers are listed in *Metals and Alloys in the Unified Numbering System*, published by the Society of Automotive Engineers (SAE International) and cosponsored by ASTM International.

<sup>†</sup> Trade name.

TABLE 1

Range and Levels of Variables in Both Natural and Coded Forms and Corresponding Response for Inhibited Solutions

Run No.	Block No.	Factors in Actual Form			Factors in Coded Form			Response
		X <sub>1</sub> , Acid Con. (M)	X <sub>2</sub> , T (°C)	X <sub>3</sub> , Inhibitor Con. (ppm)	Acid Con.	T	Inhibitor Con.	i <sub>corr</sub> (μA/cm <sup>2</sup> )
3	I	0.1	25	20	-1	-1	-1	24
7		1	25	20	+1	-1	-1	32
1		0.1	45	20	-1	+1	-1	115
8		1	45	20	+1	+1	-1	131
2		0.1	25	200	-1	-1	+1	19
11		1	25	200	+1	-1	+1	30
10		0.1	45	200	-1	+1	+1	41
6		1	45	200	+1	+1	+1	45
9		0.55	35	110	0	0	0	37
12		0.55	35	110	0	0	0	31
5		0.55	35	110	0	0	0	32
4		0.55	35	110	0	0	0	30
15	II	0.1	35	110	-1	0	0	28
14		1	35	110	+1	0	0	33
18		0.55	25	110	0	-1	0	25
17		0.55	45	110	0	+1	0	51
13		0.55	35	20	0	0	-1	51
16		0.55	35	200	0	0	+1	25

TABLE 2

ANOVA Test for Model Based on Two-Level Factorials Design

Source	Sum of Squares	Degree of Freedom	Mean Squares	F-Value	Prob>F	
Model	12,421.0	4	3,105.3	172.5	<0.0001	Significant
X <sub>1</sub> – Acid con.	242.0	1	242.0	13.4	0.015	“
X <sub>2</sub> – Temperature	6,160.5	1	6,160.5	342.3	<0.0001	“
X <sub>3</sub> – Inhibitor con.	3,280.5	1	3,280.5	182.3	<0.0001	“
X <sub>2</sub> X <sub>3</sub> – Temperature × inhibitor con.	2,738.0	1	2,738.0	152.1	<0.0001	“
Curvature	1,232.7	1	1,232.7	68.5	0.0002	Significant
Residuals	108.0	6	18.0	—	—	—
Lack of fit	79.0	3	23.3	2.7	0.2162	Not significant
Pure error	29.0	3	9.7	—	—	—

tors like hydrodynamic flow and immersion time that would surely manipulate the inhibitor effectiveness were not taken into account.

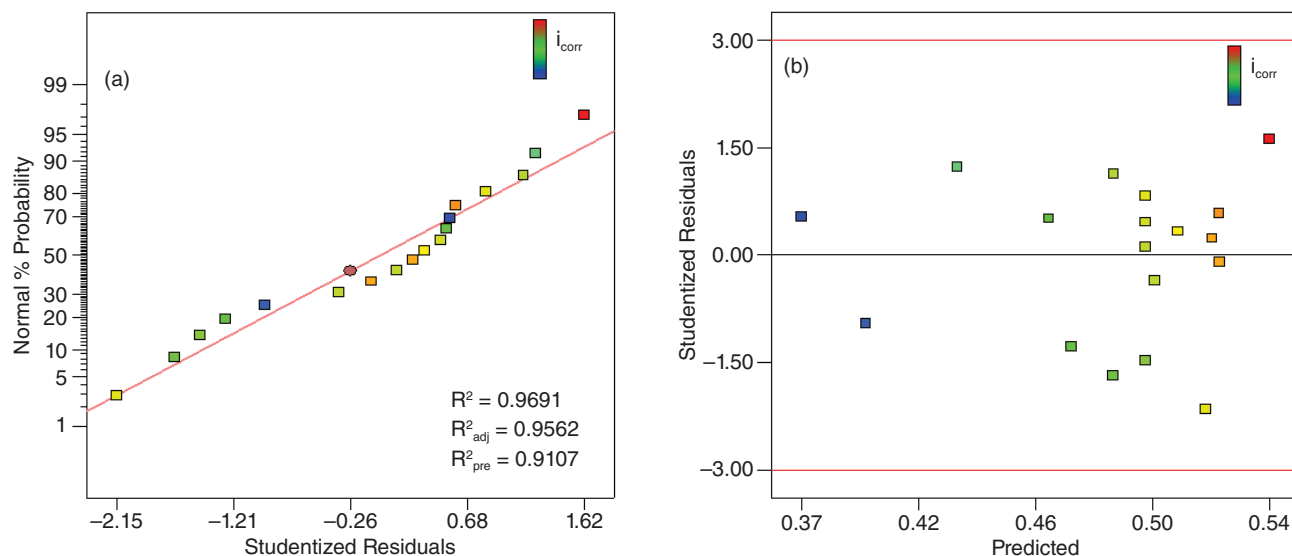
At first, a full two-level factorial design was used to investigate factors that may have a significant effect on the mild steel corrosion rate as the response value. As known, this method considers the factors only at two levels: low and high level (-1 and +1). In the use of a full two-level factorial design, a linear relation is assumed between the factor effects. Perfect linearity is not mandatory and this method will work quite well even when the linearity assumption only approximately holds.<sup>20</sup> However, there is a method of replicating the center point (a design point in the middle of each factor), which will provide protection against curvature. In addition, it allows an independent estimation of the obtained error.<sup>20,22</sup> In this way, some replicates at center point are added to the two-level factorial design.

Table 1 shows the range and the levels of the variables in both natural and coded forms, and also

the corrosion current densities ( $i_{\text{corr}}$ ) pertaining to each point. The data were collected by conducting the experiments in a random order of run numbers. There were 8 runs without any replication at design points and also 4 replicates at the center point for ANOVA to run, which have been presented as Block I. Table 2 represents the ANOVA test for the data corresponding to Block I. As can be seen, temperature, acid, and inhibitor concentrations were significant factors, and there was an interaction between temperature and inhibitor concentration factors. The F-value of 68.5 implies the presence of a significant curvature in the design space. There was a 0.01% chance that a curvature F-value with a large value could occur as a result of the noise. Consequently, the linearity assumption should not be applied. In this case, the linear relation and interaction were not capable of predicting the response accurately.<sup>20</sup> Thus, a second- or higher-order response surface model was necessary to approximate the surface around a curvature. Generally, a second-order response surface model (quadratic terms) is

**TABLE 3**  
ANOVA Test for Selected Factorial Model for Inhibited Solutions

Source	Sum of Squares	Degree of Freedom	Mean Squares	F-Value	P-Value	
Model	0.035	5	$7.017 \times 10^{-3}$	75.25	<0.0001	Significant
$X_1$ – Acid con.	$1.365 \times 10^{-3}$	1	$1.365 \times 10^{-3}$	14.64	0.0024	“
$X_2$ – Temperature	0.022	1	0.022	231.68	<0.0001	“
$X_3$ – Inhibitor con.	$7.354 \times 10^{-3}$	1	$7.354 \times 10^{-3}$	78.86	<0.0001	“
$X_2 X_3$ – Temperature $\times$ inhibitor con.	$2.566 \times 10^{-3}$	1	$2.566 \times 10^{-3}$	27.52	0.0002	“
$X_2^2$ – Temperature <sup>2</sup>	$2.197 \times 10^{-3}$	1	$2.197 \times 10^{-3}$	23.56	0.0004	“
Residuals	$1.119 \times 10^{-3}$	13	$9.325 \times 10^{-5}$	—	—	—
Lack of fit	$8.672 \times 10^{-4}$	9	$9.636 \times 10^{-5}$	1.15	0.5088	Not significant
Pure error	$2.517 \times 10^{-4}$	3	$8.391 \times 10^{-5}$	—	—	—



**FIGURE 1.** Adequacy of the regression model for inhibited solutions. (a) Normal probability plot of the studentized residuals to check for normality of residuals; (b) studentized residuals versus predicted values to check for constant error.

adequate, which can be represented by the following equation:<sup>20</sup>

$$Y = \beta_0 + \sum_{i=1}^k \beta_i X_i + \sum_{i=1}^k \beta_{ii} X_i^2 + \sum_{i=1}^{k-1} \sum_{j=1}^k \beta_{ij(i < j)} X_i X_j + \varepsilon_i \quad (1)$$

where  $Y$  is the response (here  $i_{corr}$ );  $X_i$  and  $X_j$  are variables ( $i$  and  $j$  range from 1 to  $k$ );  $\beta_0$  is the model intercept coefficient; and  $\beta_i$ ,  $\beta_{ij}$ , and  $\beta_{ii}$  are the regression coefficient of independent variable, linear interaction coefficients, and quadratic terms, respectively. In addition,  $k$  is the number of independent parameters and  $\varepsilon_i$  is the error.

In order to estimate the second-order terms in model, six points were added to the experiments according to CCFD.<sup>24,36</sup> Table 1 represents the additional tests to estimate the mathematical model containing quadratic terms as Block II. The data were analyzed so that all of the possible terms that could be placed in the model were first considered. While selecting an

appropriate transformation, which gives the best fit of model, the significance of all of the parameters was also being checked. Afterward, insignificant terms were removed from the model so that the lack-of-fit parameter was not significant. The corresponding ANOVA for the final model has been presented in Table 3. As stated, statistical testing of the model was done by F-test for ANOVA. The F-value in this table is the ratio of mean square because of regression to the mean square of the real error. If a model is a good predictor of the experimental data, the calculated F-value should be as large as possible. The model F-value of 172.5 implies the model is significant. Statistically, there is only a 0.01% chance that such a large F-value could occur because of the noise. P-values less than 0.05 indicate model terms that are significant at the probability level of 95%. Values greater than 0.1 indicate that the model terms are not significant.

The normal error distribution was confirmed by plotting the normal probability plot of the studentized residual for the model (Figure 1[a]). Also, the constant

**TABLE 4**  
Range and Levels of Variables in Both Natural and Coded Forms  
and Corresponding Response for Uninhibited Solutions

Run No.	Factors in Actual Form		Factors in Coded Form		Response
	X <sub>1</sub> , Acid Con. (M)	X <sub>2</sub> , Temperature (°C)	Acid Con.	Temperature	i <sub>corr</sub> (μA/cm <sup>2</sup> )
10	0.1	25	-1	-1	82
6	1	25	+1	-1	104
9	0.1	45	-1	+1	201
3	1	45	+1	+1	668
4	0.1	35	-1	0	122
11	1	35	+1	0	252
2	0.55	25	0	-1	92
12	0.55	45	0	+1	395
5	0.55	35	0	0	182
8	0.55	35	0	0	165
1	0.55	35	0	0	171
7	0.55	35	0	0	163

**TABLE 5**  
ANOVA Test for Selected Factorial Model for Uninhibited Solutions

Source	Sum of Squares	Degree of Freedom	Mean Squares	F-Value	P-Value	
Model	0.019	3	6.185×10 <sup>-3</sup>	561.81	<0.0001	Significant
X <sub>1</sub> – Acid Con.	3.496×10 <sup>-3</sup>	1	3.496×10 <sup>-3</sup>	317.53	<0.0001	
X <sub>2</sub> – Temperature	0.014	1	0.014	1,299.94	<0.0001	
X <sub>1</sub> X <sub>2</sub> – Acid con. × temperature	7.480×10 <sup>-4</sup>	1	7.48×10 <sup>-4</sup>	67.94	<0.0001	
Residuals	8.807×10 <sup>-5</sup>	9	1.101×10 <sup>-5</sup>			
Lack of fit	5.063×10 <sup>-5</sup>	5	1.013×10 <sup>-5</sup>	0.81	0.6101	Not significant
Pure error	3.744×10 <sup>-5</sup>	3	1.248×10 <sup>-5</sup>			

error assumption at different levels was checked at Figure 1(b) by plotting the studentized residual vs. the predicted response as obtained from the model. As can be seen, an early constant error was observed through the response range. After statistically testing the model, the obtained regression model, which predicts corrosion rate as a function of different variables, could be given in natural form as follows:

$$(i_{\text{corr}})^{-0.2} = 0.44710 - 0.025967 X_1 + 8.72601 \times 10^{-3} X_2 - 3.95138 \times 10^{-4} X_3 + 1.98984 \times 10^{-5} X_2 X_3 - 2.22326 \times 10^{-4} X_2^2 \quad (2)$$

As presented in Figure 1(a), the values of R<sup>2</sup> and R<sup>2</sup><sub>adj</sub> were quite close to 1.0, which is favorable. This means that the regression model provided an excellent explanation of the relationship between the independent variables (factors) and the response (corrosion rate). The R<sup>2</sup> value gave emphasis that 96.77% of the variability in the response could be obtained by the model, which means the model did not explain only 3.23% of the total variation. The value of adjusted determination coefficient also was high and was an indication for high significance of the model. In addition, a good correlation between the response predicted by the model and obtained by experiments was proven by the high value of R<sup>2</sup><sub>pre</sub>.

### Uninhibited Solutions

In the previous section, a mathematical model was established to predict the corrosion rate of mild steel in the inhibited solutions at various conditions. In order to estimate inhibitor efficiency, another model needed to be acquired that could estimate the corrosion rate in the uninhibited solutions. Therefore, RSM according to CCFD was again employed to design the required experiments.

Table 4 represents the designed experiments at different points and the corresponding corrosion rate. In total, there were 12 tests to run: 4 runs at the design point, 4 runs at the star point (face-centered point), and 4 points at the center point. During the data analysis, a transformation similar to that used for the model in presence of inhibitor was selected for i<sub>corr</sub>. Table 5 represents the ANOVA test for the preferred model. Considering too small of p-value, acid concentration and temperature were significant, and the acid-temperature interaction had a great impact. In addition, the lack-of-fit parameter was not significant; thus, this confirmed that other parameters not considered in the model do not have the required adequacy. Additionally, the normal error distribution and the constant error assumption were confirmed by plotting the normal probability plot of the studentized residual and the studentized residual vs. predicted

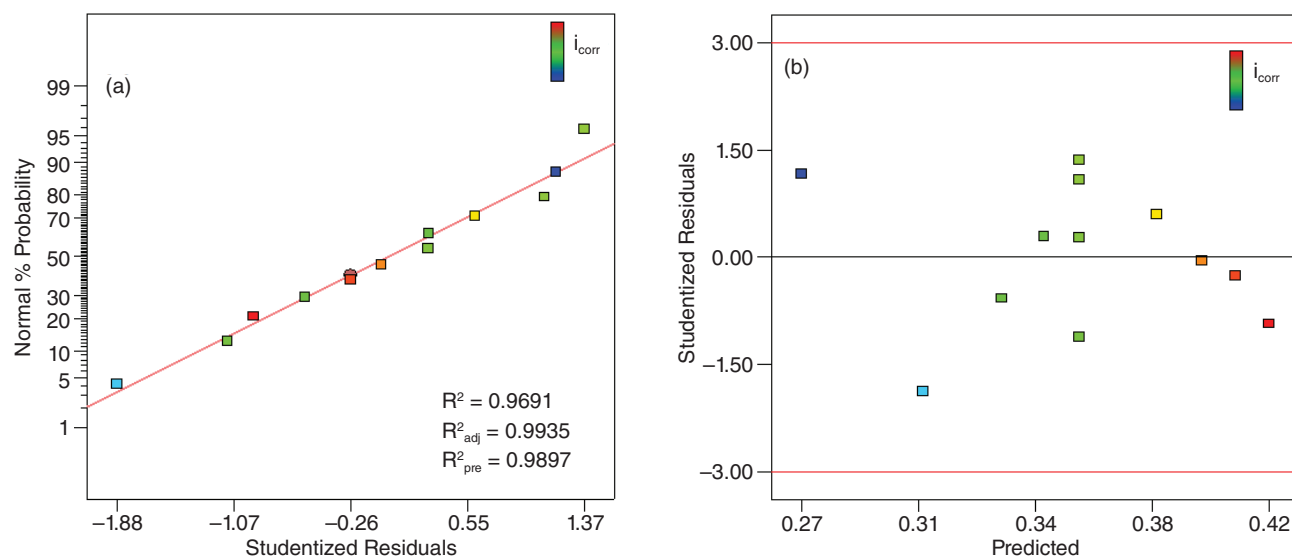


**FIGURE 2.** Adequacy of the regression model for uninhibited solutions. (a) Normal probability plot of the studentized residuals to check for normality of residuals; (b) studentized residuals versus predicted values to check for constant error.

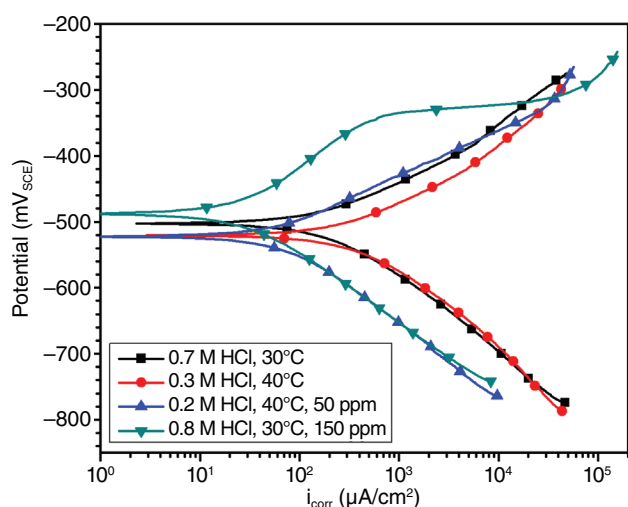


**FIGURE 3.** Polarization curves of mild steel at check points in order to test models' reliability.

**TABLE 6**

Confidence Intervals Constructed by Models and  $i_{\text{corr}}$  Estimated from Polarization Curves at Check Points

Type	Confidence Interval	Check Point	Checked
0.7 M, 30°C	$120 \leq x \leq 148$	142	OK
0.3 M, 40°C	$178 \leq x \leq 204$	192	"
0.2 M, 40°C, 50 ppm	$46 \leq x \leq 56$	53	"
0.8 M, 30°C, 150 ppm	$22 \leq x \leq 32$	25	"

response as obtained from the model (Figure 2). The  $R^2$  and  $R^2_{\text{adj}}$  value, presented in Figure 2(a), were too close to 1.0, promising an accurate model for prediction of corrosion rate. The  $R^2$  value of 99.51% showed only 0.49% of the total variation in the model. Also,

a good correlation between the response predicted by the model and obtained by experiments was verified by the high value of  $R^2_{\text{pre}}$ . After statistical evaluation and checking the accuracy, the corresponding model could be expressed as below:

$$(i_{\text{corr}})^{-0.2} = 0.49867 + 0.052721 X_1 - 3.21247 \times 10^{-3} X_2 - 3.03886 \times 10^{-3} X_1 X_2 \quad (3)$$

### The Test of Models' Reliability

The acquired models can provide confidence intervals to estimate the corrosion rate of mild steel at each point of the design space. The following formula can be used to construct the 95% confidence interval:<sup>20</sup>

$$y - t_{\alpha/2, (n-1)} \frac{S}{\sqrt{n}} \leq \mu \leq y + t_{\alpha/2, (n-1)} \frac{S}{\sqrt{n}} \quad (4)$$

In this expression,  $y$  is the response value predicted by model (herein corrosion rate),  $\alpha$  is confidence parameter (herein  $\alpha = 0.05$ ),  $n$  is the number of replicate (herein the number of replicate at center point), and  $S$  is standard deviation estimated by data acquired at center points. In addition,  $t_{\alpha/2, (n-1)}$  is the value of Student's  $t$ -distribution for  $\alpha/2$  and  $(n-1)$ .

In order to check the accuracy of models in predicting the response at non-designed points, some random points at the design space were selected. Figure 3, depicts the polarization curves at random points to check the model accuracy. Table 6 represents the  $i_{\text{corr}}$  at check points and also the confidence intervals constructed by Equation (4). As can be seen, all of the corrosion rates measured by polarization test lay in the estimated intervals. This confirms that the obtained models are accurate enough to predict the mild steel corrosion rate at the investigated levels.

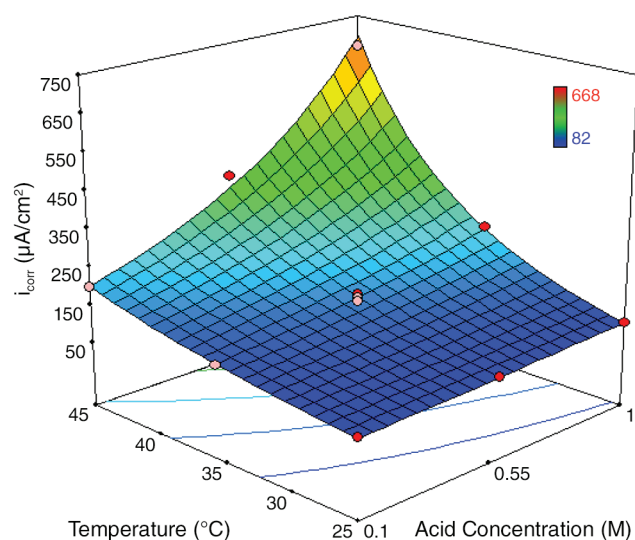


**FIGURE 4.** Response surface for mild steel corrosion rate in uninhibited solutions based on Equation (3).

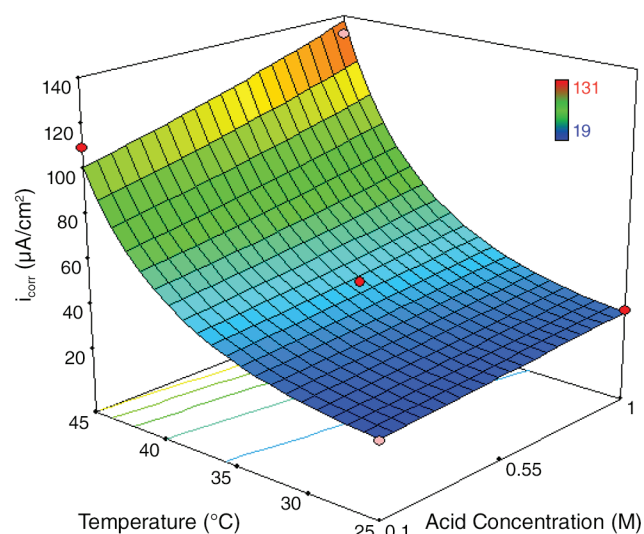


**FIGURE 5.** Response surface for  $i_{\text{corr}}$  in inhibited solutions based on Equation (2) at 20 ppm concentration.

## DISCUSSION

The surface plots can be constructed to assess the relationship between various independent variables and the considered response. Figure 4 depicts the effect of acid concentration and temperature on mild steel corrosion rate in absence of inhibitor. As can be seen, acid concentration has an insignificant effect on  $i_{\text{corr}}$  when the temperature is low. But, simultaneously raising temperature and acid concentration gives rise to a considerable increase in corrosion rate. In other words, the effect of acid concentration, which determines both pH value and chloride ion concentration, is fortified by the temperature. This effect refers to more chemical adsorption of  $\text{Cl}^-$  ions into the surface when the temperature increases, resulting in more anodic dissolution of iron by catalytic effect of chloride ions.<sup>7,15,18</sup>

The simultaneous effect of acid concentration and temperature on  $i_{\text{corr}}$  has been shown in Figure 5 in presence of 20 ppm 4ATP. As can be seen, with increasing acid concentration at low temperature, the corrosion rate does not change significantly. However, a slight increase is observed in the corrosion rate with rising acid concentration at the elevated temperatures. This suggests that the negative effect of acid concentration can be impeded by an inhibitor even at low concentration. As known, the adsorption of inhibitor molecules into the surface decreases the active area exposed to the corrosive solution in such a way that more adsorption of  $\text{Cl}^-$  ions and water molecules can be adequately prevented by inhibitor molecules.<sup>14,19,35</sup>

Figure 6 illustrates the surface plots of  $i_{\text{corr}}$  as a function of inhibitor concentration and temperature. As it is observed, the temperature intensively increases the corrosion rate. It is valuable that inhibitor

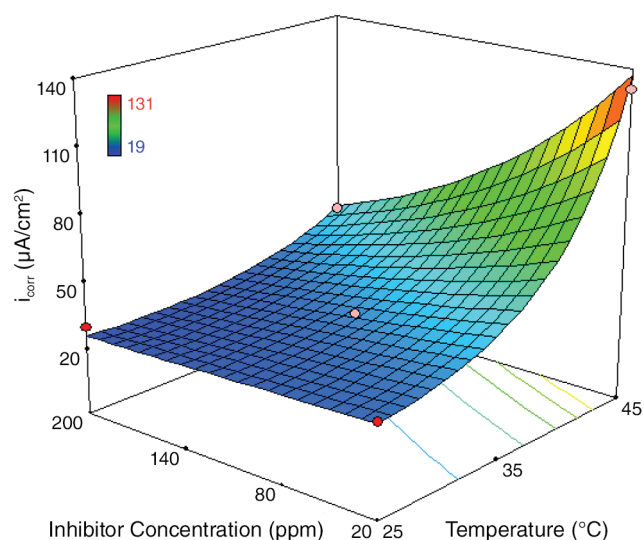


**FIGURE 6.** Response surface for mild steel corrosion rate in 1 M HCl inhibited solutions based on Equation (2).

concentration considerably diminishes the destructive effect of temperature. This fact is more obvious when in presence of 200 ppm 4ATP: the ascending trend of  $i_{\text{corr}}$  with increasing temperature turns into a nearly flat line. As known, the temperature facilitates the iron dissolution in acidic media but the surface blocking with more inhibitor molecules can slow down the corrosion rate. Although temperature always increases  $i_{\text{corr}}$ , the decreased intensity of  $i_{\text{corr}}$  with increasing inhibitor concentration is more considerable when the temperature is low. This suggests that lower inhibitor concentration can adequately reduce the corrosion so that further addition is not cost-effective, which is very important from a practical point of view when the temperature is low.

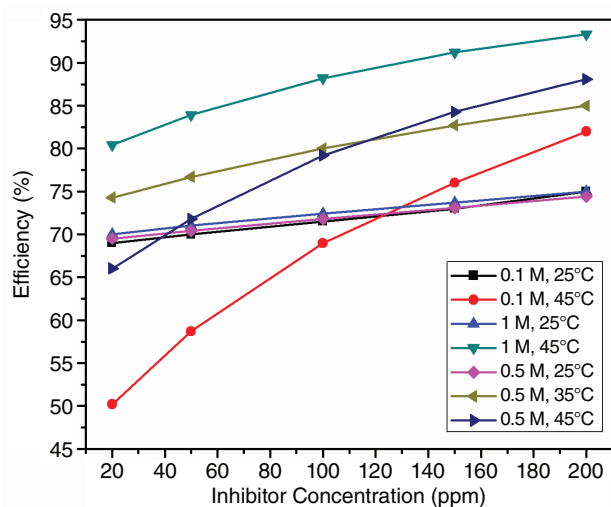


FIGURE 7. Efficiency of 4ATP calculated in various conditions.

The surface coverage ( $\theta$ ) and inhibitor efficiency ( $\% \eta$ ) are parameters that are widely used to evaluate inhibitive performance of organic compounds in different conditions. In the present work, the obtained mathematical models are responsible for estimating  $i_{\text{corr}}$  in absence and presence of inhibitor at each point of design space. As a result, surface coverage and inhibitor efficiency can be calculated with the following equations using the estimated corrosion current densities in absence ( $i_{\text{corr}}^0$ ) and presence of inhibitor ( $i_{\text{corr}}$ ) at each point.<sup>37</sup>

$$\theta = \frac{i_{\text{corr}}^0 - i_{\text{corr}}}{i_{\text{corr}}^0} \quad (5)$$

$$\% \eta = \theta \times 100 \quad (6)$$

Figure 7 shows the efficiency 4ATP as a function of inhibitor concentration in various conditions. It is remarkable that highest efficiency is obtained when acid concentration and temperature are at their highest level. This phenomenon refers to the more enhanced value in the corrosion rate by simultaneously increasing acid concentration and temperature in blank solutions, compared to the inhibited solutions. Thus, the enhanced efficiency must not be interpreted as improvement in adsorption performance. When the solution is 0.1 M at 45°C, the efficiency is at lowest obtained value but it shows an ascending trend with increasing inhibitor concentration and reaches 80%

at 200 ppm. Although, the temperature gives rise to increasing the corrosion rate in both the inhibited and uninhibited solutions, the increased value is further at low inhibitor concentrations in comparison with blank solutions, resulting in a decrease in efficiency. While at a higher concentration, the inhibitor can noticeably slow down the corrosion rate, which can be observed as enhanced inhibitor efficiency. Comparison of efficiency at 25°C reveals that the acid concentration has no considerable effect on efficiency so that efficiency slightly increases with rising inhibitor concentration. In addition, efficiency evaluation in 0.5 M HCl shows that the temperature has a positive effect on the efficiency of 4ATP for mild steel. This could not be regarded as an enhancement in inhibitor adsorption because the improved efficiency basically results from the increased corrosion rate of mild steel in uninhibited solutions.

The adsorption isotherms provide important information on interaction between the inhibitor and the metal surface. Langmuir isotherm is generally applied because the inhibitors mostly obey this isotherm.<sup>10,16,35,38-41</sup> According to Langmuir isotherm, there is a relation between the surface coverage,  $\theta$ , and inhibitor concentration in mol/L,  $C$ , as follows:<sup>15,37</sup>

$$\frac{C}{\theta} = \frac{1}{K_{\text{ads}}} + C \quad (7)$$

Considering Equation (7), the value of equilibrium constant,  $K_{\text{ads}}$ , is calculated from the reciprocal of the intercept of  $C/\theta$ -axis. Afterward, the standard free energy of inhibitor adsorption,  $\Delta G_{\text{ads}}^0$ , on metal surface can be calculated using following equation:<sup>37</sup>

$$\Delta G_{\text{ads}}^0 = -RT \ln(55.5 K_{\text{ads}}) \quad (8)$$

In this expression,  $R$  is the gas constant,  $T$  is the absolute temperature, and 55.5 is the molar concentration of water in 1 L solution.

The acquired mathematical models make it possible to calculate the standard free energy of adsorption,  $\Delta G_{\text{ads}}^0$ , for 4ATP in different acid concentrations and temperatures. The  $\Delta G_{\text{ads}}^0$  values have been given in Table 7. As can be seen, all of the  $\Delta G_{\text{ads}}^0$  are nearly similar and the adsorption mechanism of 4ATP on the mild steel surface in HCl solution probably involves both physisorption and chemisorption.<sup>10,35,37</sup> In other words, the adsorption type of 4ATP into the metal surface is invariable in HCl solutions, while inhibitor

TABLE 7

The Calculated  $\Delta G_{\text{ads}}^0$  Based on Langmuir Adsorption Isotherm in Different Acid Concentrations and Temperatures

Solution Temperature (°C)	0.1 M HCl			0.5 M HCl			1 M HCl		
	25	35	45	25	35	45	25	35	45
$\Delta G_{\text{ads}}^0$ (kJ mol <sup>-1</sup> )	-36.76	-36.02	-34.97	-36.75	-36.95	-36.32	-36.76	-37.99	-38.15



efficiency is altered with change in acid concentration and temperature. This suggests that 4ATP directly adsorbs into the metallic surface from suitable adsorption sites existing in molecular structures like sulfur and nitrogen atoms. It should be noted that  $\Delta G_{\text{ads}}^0$  obtained for 4ATP in 0.1 M HCl solution and at 25°C is equal, as obtained in previous work.<sup>35</sup> Thus, it may be deduced that 4ATP has a different efficiency for various types of mild steel but the type of adsorption will remain constant in a similar acidic solution.

## CONCLUSIONS

❖ The response surface method is a good method to evaluate the inhibitive performance of organic compounds in different environmental conditions. RSM presents tridimensional plots which provide good insight in order to analyze and discuss the acquired results. Also, it reduces the number of experimental runs required for comprehensive evaluation of inhibitor performance, leading to the minimizing of cost and time of experimentation. A more important benefit is that RSM also allows investigating the effect of one variable at several levels of other factors. The mathematical models can be acquired to estimate the corrosion rate in various circumstances and provide the possibility of the calculation of inhibitors' efficiency and also their adsorption isotherms at different conditions. As an example of an application, three effects of temperature, acid, and inhibitor concentrations on inhibitive behavior of 4ATP for mild steel were studied. Two mathematical models were established in order to estimate mild steel corrosion rate in the inhibited and uninhibited solutions, and the efficiency in various conditions was calculated. The adsorption energy was calculated using Langmuir isotherm in different conditions. The results showed that the efficiency changes in various conditions, but the adsorption type remains constant.

## ACKNOWLEDGMENTS

Authors appreciate the financial support from Ferdowsi University of Mashhad provision of laboratory facilities during the period that this research was conducted. Mr. Hoseinpoor is also appreciated for his kind help.

## REFERENCES

1. Z. Ahmad, B.J. Abdul Aleem, *Mater. Des.* 23, 2 (2002): p. 173-180.
2. M.K. Awad, M.S. Metwally, S.A. Soliman, A.A. El-Zomrawy, M.A. Bedair, *J. Ind. Eng. Chem.* 20, 3 (2014): p. 796-808.
3. H. Ezuber, A. El-Houd, F. El-Shawesh, *Mater. Des.* 29, 4 (2008): p. 801-805.
4. M. Finšgar, J. Jackson, *Corros. Sci.* 86 (2014): p. 17-41.
5. B. Jugović, M. Gvozdenović, J. Stevanović, T. Trišović, B. Grgur, *Mater. Des.* 30, 8 (2009): p. 3291-3294.
6. E. McCafferty, *Introduction to Corrosion Science* (New York, NY: Springer, 2010).
7. M. Vakili Azghandi, A. Davoodi, G.A. Farzi, A. Kosari, *Metall. Mater. Trans. A* 44, 12 (2013): p. 5493-5504.
8. J. Weber, *Mater. Des.* 4, 2 (1983): p. 723-727.
9. Y. Xie, L. Xu, C. Gao, W. Chang, M. Lu, *Mater. Des.* 36 (2012): p. 54-57.
10. F. Bentiss, M. Lagrenee, M. Traisnel, J.C. Hornez, *Corros. Sci.* 41 (1999): p. 789-803.
11. V. Sastri, *Corrosion Inhibitors: Principles and Applications* (Hoboken, NJ: John Wiley & Sons, Inc., 2011).
12. G. Tansuğ, T. Tüken, E.S. Giray, G. Findikkıran, G. Sığirek, O. Demirkol, M. Erbil, *Corros. Sci.* 84 (2014): p. 21-29.
13. M. Vakili Azghandi, A. Davoodi, G.A. Farzi, A. Kosari, *Corros. Sci.* 64 (2012): p. 44-54.
14. M. Finšgar, D. Kek Merl, *Corros. Sci.* 83 (2014): p. 164-175.
15. A. Kosari, M.H. Moayed, A. Davoodi, R. Parvizi, M. Momeni, H. Eshghi, H. Moradi, *Corros. Sci.* 78 (2014): p. 138-150.
16. I.B. Obot, E.E. Ebenso, M.M. Kabanda, *J. Environ. Chem. Eng.* 1, 3 (2013): p. 431-439.
17. A. Ongun Yüce, B. Dođru Mert, G. Kardaş, B. Yazıcı, *Corros. Sci.* 83 (2014): p. 310-316.
18. A.K. Singh, M.A. Quraishi, *Corros. Sci.* 52 (2010): p. 152-160.
19. R. Solmaz, *Corros. Sci.* 52 (2010): p. 3321-3330.
20. D.C. Montgomery, *Design and Analysis of Experiments* (New York, NY: Wiley, 2001).
21. G. Annadurai, R.-S. Juang, D.-J. Lee, *Adv. Environ. Res.* 6, 2 (2002): p. 191-198.
22. K. Mahdi, R. Gheshlaghi, G. Zahedi, A. Lohi, *J. Petrol. Sci. Eng.* 61, 2-4 (2008): p. 116-123.
23. V.S. Aigbodion, S.B. Hassan, *Mater. Des.* 31, 4 (2010): p. 2177-2180.
24. N. Bursali, S. Ertunc, B. Akay, *Chem. Eng. Process. Process. Intensif.* 45, 11 (2006): p. 980-989.
25. M. Poroč-Seritan, S. Gutt, G. Gutt, I. Cretescu, C. Cojocaru, T. Severin, *Chem. Eng. Res. Des.* 89, 2 (2011): p. 136-147.
26. B. Tansel, B. Pascual, *Desalination* 169, 1 (2004): p. 1-10.
27. N. Aslan, *Powder Technol.* 185, 1 (2008): p. 80-86.
28. S.C. Vettivel, N. Selvakumar, R. Narayanasamy, N. Leema, *Mater. Des.* 50 (2013): p. 977-996.
29. V.I. Vitanov, N. Javaid, D.J. Stephenson, *Surf. Coatings Technol.* 204, 21-22 (2010): p. 3501-3508.
30. M. Balachandran, S. Devanathan, R. Muraleekrishnan, S.S. Bhagawan, *Mater. Des.* 35 (2012): p. 854-862.
31. B. Oraon, G. Majumdar, B. Ghosh, *Mater. Des.* 27 (2006): p. 1035-1045.
32. B. Oraon, G. Majumdar, B. Ghosh, *Mater. Des.* 28, 7 (2007): p. 2138-2147.
33. B. Oraon, G. Majumdar, B. Ghosh, *Mater. Des.* 29, 7 (2008): p. 1412-1418.
34. Y. Tan, M. Guo, L. Cao, L. Zhang, *Constr. Build. Mater.* 47 (2013): p. 799-805.
35. A. Kosari, M. Momeni, R. Parvizi, M. Zakeri, M.H. Moayed, A. Davoodi, H. Eshghi, *Corros. Sci.* 53 (2011): p. 3058-3067.
36. S. Pongstabodee, S. Monyanon, A. Luengnaruemitchai, *Int. J. Hydrogen Energy* 37, 6 (2012): p. 4749-4761.
37. J. Aljourani, K. Raeissi, M.A. Golozar, *Corros. Sci.* 51 (2009): p. 1836-1843.
38. K.R. Ansari, M.A. Quraishi, A. Singh, *Corros. Sci.* 79 (2014): p. 5-15.
39. M.A. Hegazy, M. Abdallah, M.K. Awad, M. Rezk, *Corros. Sci.* 81 (2014): p. 54-64.
40. G.I. Ostapenko, P.A. Gloukhov, A.S. Bunev, *Corros. Sci.* 82 (2014): p. 265-270.
41. R. Yildiz, A. Döner, T. Dođan, I. Dehri, *Corros. Sci.* 82 (2014): p. 125-132.